

# Morphology and Coalescence of Ethylene Copolymers: Influence of Thermal Treatments and Sorbitol Nucleating Agents

W. Lin,\* C. T. Bellehumeur

Department of Chemical and Petroleum Engineering, Schulich School of Engineering, University of Calgary, Calgary, Alberta, Canada T2N 1N4

Received 11 May 2006; accepted 12 June 2006

DOI 10.1002/app.25081

Published online in Wiley InterScience (www.interscience.wiley.com).

**ABSTRACT:** Coalescence of polymer particles is a key phenomenon in many powder processing technologies. Both the extent and the rate of coalescence between particles govern the production cycle and the performance of the end-product. It is well accepted that both processing conditions and material formulation affect the morphology of molded parts and consequently their mechanical properties. The interest of this study is to evaluate the impact that changes in morphological features caused by the imposition of different thermal treatments as well as by the addition of a nucleating agent (bis 3,4 dimethylbenzylidene sorbitol) have on the coalescing behavior of ethylene copolymers produced from Ziegler–Natta and metallocene catalyst technologies. Results showed that samples produced using slower cooling rates exhibited higher crystallinity and increased thermal stability. Variations in thermal treatments, however, only resulted

in minor changes in the coalescing behavior of the resins considered in this work. However, the addition of the nucleating agent to Ziegler–Natta ethylene copolymers led to the formation of crystalline structures with increased material thermal stability, but reduced chain mobility, and consequently resulted in a slower coalescing rate. These effects, however, are dependent on the molecular structure of the copolymers. The addition of the sorbitol nucleating agent influenced the morphological structure of the metallocene copolymer used in this work but did not result in any significant changes in the coalescence behavior of the resin. © 2006 Wiley Periodicals, Inc. *J Appl Polym Sci* 102: 5443–5455, 2006

**Key words:** sintering; rotational molding; crystallization; nucleating agent; LLDPE

## INTRODUCTION

The coalescence of polymeric materials, also referred to as sintering, is a phenomenon encountered in several industrial applications such as rotational molding, powder coating, and rapid prototyping. This phenomenon influences both the molding cycle and the properties of the final parts. Resins with poor coalescence behavior require a longer heating time in the molding cycle or the result is the production of parts with large and numerous bubbles, which negatively impact the properties and appearance of the final product. The coalescence of polymers is driven by the work of surface tension and counteracted by the viscous dissipation associated with the molecular diffusion within the coalescing domain. It is well established that the zero-shear viscosity, material elasticity, and surface tension play an important role in determining coales-

cence behavior in the rotational molding process. Changes in the material formulation can be implemented to maximize the coalescing behavior through these properties. Such changes can also have important repercussions on the physical, chemical, and mechanical performance of the molded parts, though changes in the morphology of the material, as demonstrated by the work of Oliveira and coworkers.<sup>1–3</sup> The reverse problem, that is to evaluate the impact that changes in the morphology has on the materials' processability has, however, seldom been investigated.

Ethylene copolymers are commercially an important class of polyethylenes and are produced through the copolymerization of ethylene and  $\alpha$ -olefins. The resulting polymers usually have a relatively linear molecular structure but a lower density, due to the presence of comonomers, and are thus referred to as linear low-density polyethylene (LLDPE). Their morphology depends on many factors such as material composition (comonomer content, comonomer type, and additives), thermal history, and molecular structure (distribution of comonomer). Among them, the comonomer content plays one of the most important roles in determining the crystallization behavior resulting morphological features. An increase in comonomer content generally results in a gradual change in the morphology of ethyl-

\*Present address: NOVA Chemicals Corporation, Calgary, Alberta, Canada T2E 7K7.

Correspondence to: C. T. Bellehumeur (cbellehu@ucalgary.ca).

Contract grant sponsor: NOVA Chemicals Corporation and the Natural Science Engineering and Research Council of Canada.

ene copolymers from well-developed spherulites to less organized fringed micellar crystals.<sup>4</sup> Meanwhile, with increasing the comonomer content, the lamellar thickness, the melting temperature, and the heat of fusion decrease, while the melting range broaden.<sup>5-8</sup> Other important characteristics are the comonomer content and distribution, which affect the length of linear ethylene sequence in the molecules. Long ethylene sequences undergo chain folding at higher temperatures, while the shorter ethylene sequences start crystallizing at lower temperatures.<sup>9</sup> Samples having a high comonomer content and heterogeneities in the comonomer distribution will typically show more than one type of crystal morphologies: chain-folded lamellae formed from long ethylene sequences and bundlelike crystals formed from the short ethylene sequences.<sup>10</sup> Variations in the thermal treatment imposed on the material during the crystallization process also show important effects on the crystallization and morphology of ethylene copolymers. Slow cooled samples normally have higher crystallinity and larger spherulites than those of quenched samples. The lamellar thickness increases significantly with decreasing cooling rate, and, furthermore, decreasing the cooling rate results in bigger spherulites. Peeters et al.<sup>11</sup> attributed the less organized supermolecular structure to the diffusion-controlled crystal growth under rapid cooling condition, as previously concluded by Mandelkern et al.<sup>12</sup> Furthermore, it was shown that the lowering of the crystallinity caused by an increase of the cooling rate is most prominent for copolymers with lower comonomer content.<sup>11,13</sup> Annealing treatments also influence the morphology of ethylene copolymers by forming more perfect crystals and shifting the melting peak of DSC thermograms to higher temperatures.<sup>14</sup> The effect of annealing treatments varies with the ethylene sequences length distributions, having less impact on the more linear polymers.<sup>15</sup>

A wide range of additives are included in the formulation of polymers and their effects on the final morphology can be very important. Among them, nucleating agents are used in semicrystalline polymer to improve mechanical properties or appearance of end-products. They contribute to increasing the rate of crystallization, as well as the degree of crystallinity and the lamellae thickness of nucleated polymers. Nucleating agents act as foothold for the generation of

nuclei. The nucleation process can be considered to be heterogeneous through the adsorption of polymer chains in the melt onto the nucleating agent surfaces, the mechanism and kinetics being governed by differences in surface free energy. It has been suggested that the nucleating ability is decided by the geometrical and dimensional similarities between the additive and the growing crystalline lattice.<sup>16-18</sup> Yet, one cannot easily identify the structural requirements for nucleating agents for polymers with different molecular structure. The selection of effective nucleating agents still heavily relies on trial and error.

This work is one part of a research program that focuses on the processability of ethylene copolymers used in rotational molding applications. The specific aim is to determine the effect of particles' morphology on the coalescence process of copolymers synthesized using Ziegler-Natta and metallocene catalyst technologies. Polymer coalescence has traditionally been studied as a flow problem. Past studies have shown that the controlling factors are the particle size, the material viscosity, and the material surface tension.<sup>19-21</sup> Recent studies have shown, however, that the material molecular structure, molecular order, and morphology are also of importance.<sup>22-25</sup> At this point, it is still unclear through which mechanism changes in the morphology influences the coalescing behavior of polymer particles.

## EXPERIMENTAL

### Materials

Results obtained for three commercial ethylene copolymers are presented in this publication: NOVAPOL<sup>®</sup> TR-0338, SCLAIR<sup>®</sup> 8107, as well as ME8166 (from Borealis). The resins will be referred as PE1, PE2, and mPE3, respectively. Molecular weight distributions were determined by high temperature gel-permeation chromatography (GPC) using a Waters 150C high temperature GPC with a differential refractive index (DRI) detector, in accordance with ASTM D6474. The material properties are presented in Table I, data being provided by suppliers unless noted otherwise.

A sorbitol nucleating agent was compounded with the resins by using a HAAKE Rheocord 40 torque rheometer equipped with a HAAKE 600 series internal batch mixer. A concentration of 0.2% (weight fraction)

TABLE I  
Material Properties of Ethylene Copolymers

| Resin | $M_w$<br>(g/mol) | $M_w/M_n$ | Density <sup>a</sup><br>(g/cm <sup>3</sup> ) | Catalyst      | Comonomer |
|-------|------------------|-----------|--|---------------|-----------|
| PE1   | 76,800           | 3.96      | 0.9380                                       | Ziegler-Natta | Hexene    |
| PE2   | 66,400           | 3.95      | 0.9240                                       | Ziegler-Natta | Butene    |
| mPE3  | 76,100           | 2.00      | 0.9402                                       | Metallocene   | Hexene    |

<sup>a</sup> Data provided by material supplier.

of Millad<sup>®</sup>3988 (DMDBS sorbitol nucleating agent, supplied by Milliken Chemical) was used to provide optimal nucleating action on the material.<sup>18</sup> Blending was performed at 190°C in a nitrogen environment for 5 min. Compounds were prepared at 190°C to minimize the extent of thermal degradation reactions that occur during processing. It was shown that, in the preparation of specimens used in coalescence experiments, poor choice of processing conditions (high temperature or high shear) can cause changes in the material properties, due to thermo-oxidative reactions, which greatly influence the coalescing behavior of the material.<sup>26</sup> While selected compounding conditions might not have been best possible to maximize the clarifying effect of DMDBS, we consider that they were optimal in preparing samples with improved clarity while minimizing the impact of this additional processing step in the preparation of our samples in the occurrence of thermal degradation reactions.

#### Sample preparation and coalescence experiments

Cylindrical particles with diameter of 500  $\mu\text{m}$  and thickness of  $310 \pm 30 \mu\text{m}$  were made by hot pressing

polymer resins into a perforated aluminum plate at 190°C. The plate was then removed from the hot press unit and subjected to different cooling conditions: severe (quenching in ice water), gradual (cooled in ambient air), and controlled (cooled in a programmable oven with a fixed cooling rate of 1°C/min). Multiple-step annealing treatments were also conducted using air-cooled cylinders, which were placed into a Lindberg/Blue GO1390PA gravity convection oven equipped with a programmable temperature controller and purged with nitrogen to prevent the occurrence of thermo-oxidative degradation reactions. The initial temperature was set several degrees lower than the resins' melting temperature: 120°C for PE1 and mPE3, 114°C for PE2. The equilibrium time at each temperature was 120 min. The temperature was lowered seven times in stages of 6°C and then cooled to 30°C.

Coalescence experiments, as illustrated in Figure 1, were performed using cylindrical particles, which were placed in close proximity on a glass slide. The glass slide was then loaded into the heating chamber of a METTLER FP82 hot stage at the initial temperature (111°C). The temperature was then ramped from

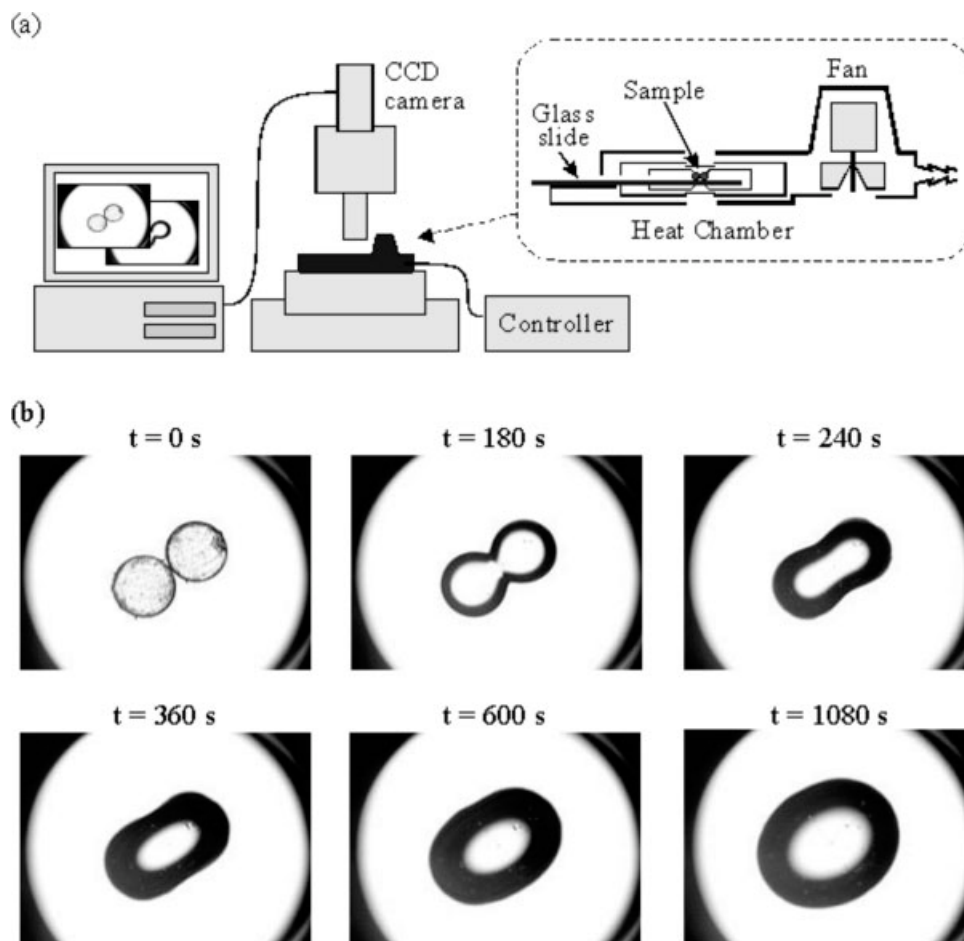


**Figure 1** Coalescence experiment: (a) Schematic of apparatus; (b) typical evolution observed for neck growth between two cylindrical particles (PE1, air-cooled cylinders).

**TABLE II**  
Rheological Properties of Ethylene Copolymers

| Resin | Zero-shear viscosity (Pa s) |          |          |
|-------|-----------------------------|----------|----------|
|       | at 150°C                    | at 170°C | at 190°C |
| PE1   | 4,750                       | 3,270    | 2,510    |
| PE2   | 4,180                       | 2,610    | 2,200    |
| mPE3  | 4,620                       | 3,290    | 2,300    |

111°C to 201°C at a rate of 5°C/min, conditions which are representative of that imposed to the material in the actual rotational molding process. A CCD camera coupled to an Olympus BX60 optical microscope was used to record the coalescence sequence and photographs were recorded at a fixed time interval. The coalescence process was quantified using the ratio of the radius of the neck formed between adjacent cylinders ( $y$ ) over the radius of the coalescing cylinders ( $a$ ). Accordingly, a value of  $y/a$  equal to 1 indicates the completion of the coalescence process. Changes in the shape of the neck and cylindrical particles were analyzed using the commercial software ImagePro<sup>®</sup>. Each experiment was repeated a minimum of four times to ensure reproducibility of results. The error bars in figures illustrating the change in dimensionless neck growth with time represent the standard deviation of the experimental data.

### Rheological characterization

The rheological measurements were carried out by using a HAAKE RS150 rotational rheometer. A parallel-plate sensor with a diameter of 20 mm was used. The shearing gap was 1.4 mm and nitrogen environment was maintained while testing. Oscillatory measurements were conducted at several temperatures and the values of the zero shear viscosity reported in Table II were estimated by fitting the modified Cross model:

$$\eta = \frac{\eta_0}{1 + (C\omega)^m} \quad (1)$$

where  $\eta$ ,  $\eta_0$ ,  $\omega$  represent the material viscosity, viscosity at low frequencies (zero-shear viscosity), and frequency, respectively, while  $C$  and  $m$  are model parameters. Additionally, dynamic mechanical analysis (DMA) was conducted with a Rheometrics dynamic spectrometer RDS-II with a cone/plate fixture configuration (diameter of 25.0 mm and the cone angle of 0.1 rad). A dynamic shear strain of 1% and a frequency of 1.0 rad/s were applied. Samples were melted at 140°C and then cooled to 80°C with a cooling rate of 1°C/min, and the changes of material viscosity were recorded.

### Thermal characterization

A Mettler 12E DSC was used to characterize the thermal behavior of all resins. This calorimeter was calibrated with an Indium standard. Approximately 5 mg of polymer sample was heated from 50°C to 150°C, keeping it isothermal for 5 min, and cooled from 150°C to 50°C; the heating/cooling rate is 10°C/min. The endotherm and exotherm curves were recorded, and the melting temperature and the crystallization temperature were obtained from the peak point of the curves. The degree of crystallinity was evaluated as the ratio between the heat of fusion of the sample and the heat of fusion of the perfect crystalline polyethylene.<sup>13</sup>

### Morphological characterization

The crystalline structures of studied polymer samples were observed using polarized light microscopy (Olympus BX60). Polymer cylinders were embedded using epoxy resin (EMBed-812). The medium was cured in an oven at 60°C for 24 h. Thin sections (12–

**TABLE III**  
Thermal Properties and Crystallite Size of Cylindrical Particles with Different Thermal History and Chemical Composition

| Resin | Treatment conditions or additives | Thermal properties <sup>a</sup> |            |                   | Crystallite size (Å) <sup>b</sup> |          |
|-------|-----------------------------------|---------------------------------|------------|-------------------|-----------------------------------|----------|
|       |                                   | $T_m$ (°C)                      | $T_c$ (°C) | Crystallinity (%) | at (110)                          | at (200) |
| PE1   | Quenched                          | 127.1                           | 113.9      | 47.2              | 219.6                             | 166.3    |
|       | Air-cooled                        | 127.5                           | 113.2      | 53.2              | 268.1                             | 198.7    |
|       | Slow-cooled                       | 129.4                           | 113.2      | 54.8              | 278.1                             | 218.4    |
|       | 0.2% DMDBS                        | 128.8                           | 117.1      | 54.8              | 258.4                             | 200.2    |
| PE2   | Quenched                          | 122.8                           | 106.1      | 36.0              | 118.4                             | 136.9    |
|       | Air-cooled                        | 122.5                           | 106.2      | 40.9              | 215.6                             | 143.1    |
|       | 0.2% DMDBS                        | 123.6                           | 113.9      | 42.3              | 214.9                             | 148.9    |
| MPE3  | Quenched                          | 126.5                           | 113.6      | 48.0              | 238.2                             | 171.4    |
|       | Air-cooled                        | 127.4                           | 113.6      | 54.7              | 263.2                             | 189.9    |
|       | 0.2% DMDBS                        | 128.2                           | 115.1      | 54.3              | 277.8                             | 193.3    |

<sup>a</sup> From DSC measurements.

<sup>b</sup> From WAXS measurements.

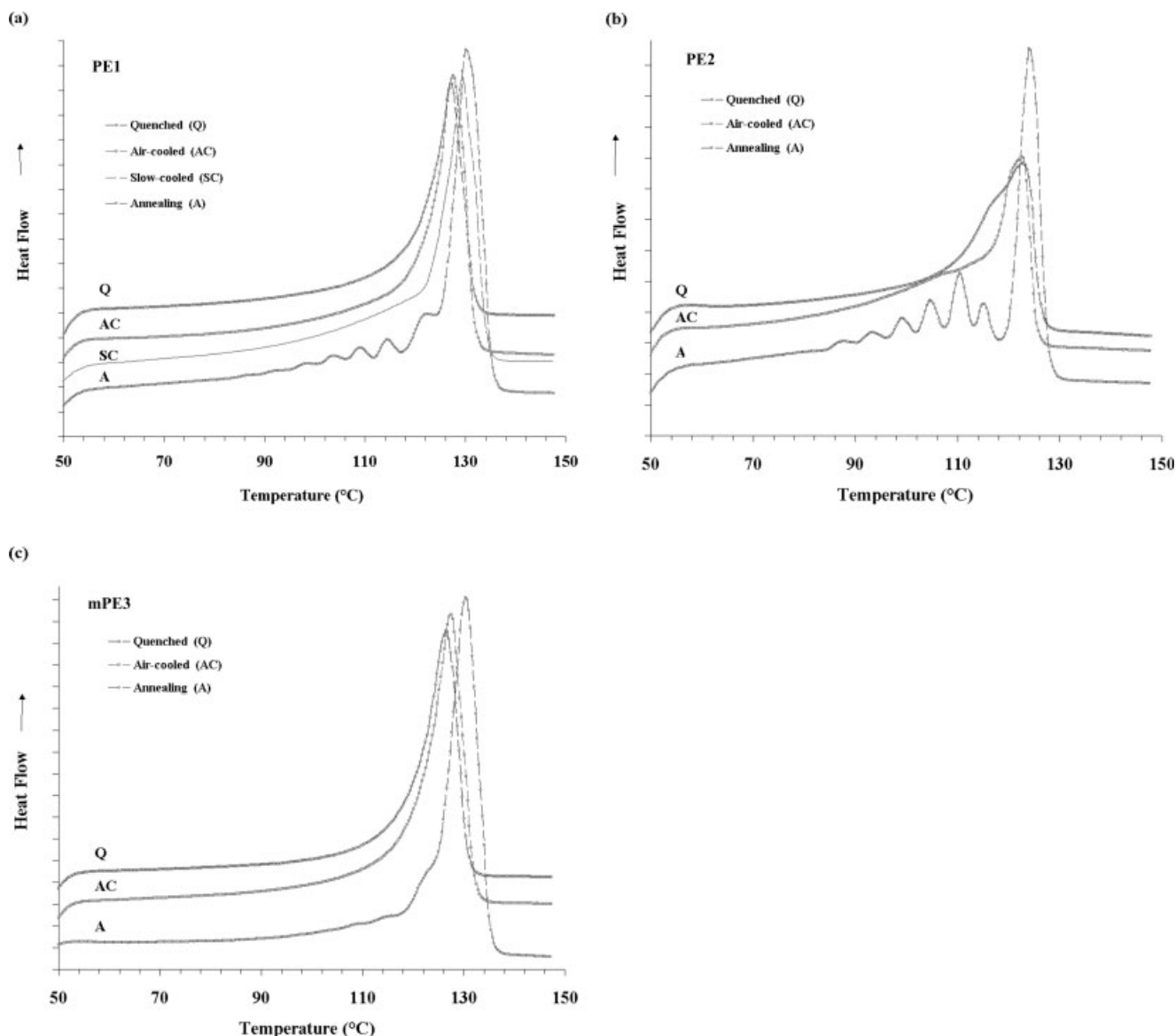


**Figure 2** DSC curves on the first heating step (an adapted scale is drawn by consecutively adding 1 unit to each curve). (a) PE1; (b) PE2; (c) mPE3.

20  $\mu\text{m}$  thickness) were cut using a LEICA RM2165 microtome equipped with glass/diamond knife. Those cross sections were sandwiched between a microscope slide and cover glass using a mounting medium (Permount<sup>®</sup>).

X-ray diffraction tests were conducted to characterize the crystalline structure of cylindrical particles using SIEMENS GADDS general area detector diffraction system. Measurements were performed at room temperature. The X-ray was produced in the X-ray tube by electron beam with 40 kV and 40 mA using  $\text{Cu K}\alpha_1$  radiation (1.541  $\text{\AA}$ ). The detector distance was 30 cm when measuring the crystallite sizes to maximize resolution and minimize peak FWHM (full width at half maximum). The angle of detector rotation ( $2\theta$ ) was  $25^\circ$ . Collection time was 600 s. A com-

mercial software DIFFRACplusProfile was used to calculate the crystallite size.

## RESULTS AND DISCUSSIONS

### Morphology of coalescing particles

#### Effect of thermal treatment

Results obtained from differential scanning calorimetry (DSC) and wide-angle X-ray scattering (WAXS) are summarized in Table III. The degree of crystallinity ( $X_c$ ), as well as the crystallite size, increased with decreasing the cooling rate. Data presented in Table III also suggests an effect of the cooling conditions on the melting temperature ( $T_m$ ) for PE1 and PE3. On the other hand, the crystallization temperature ( $T_c$ ) did not vary appre-

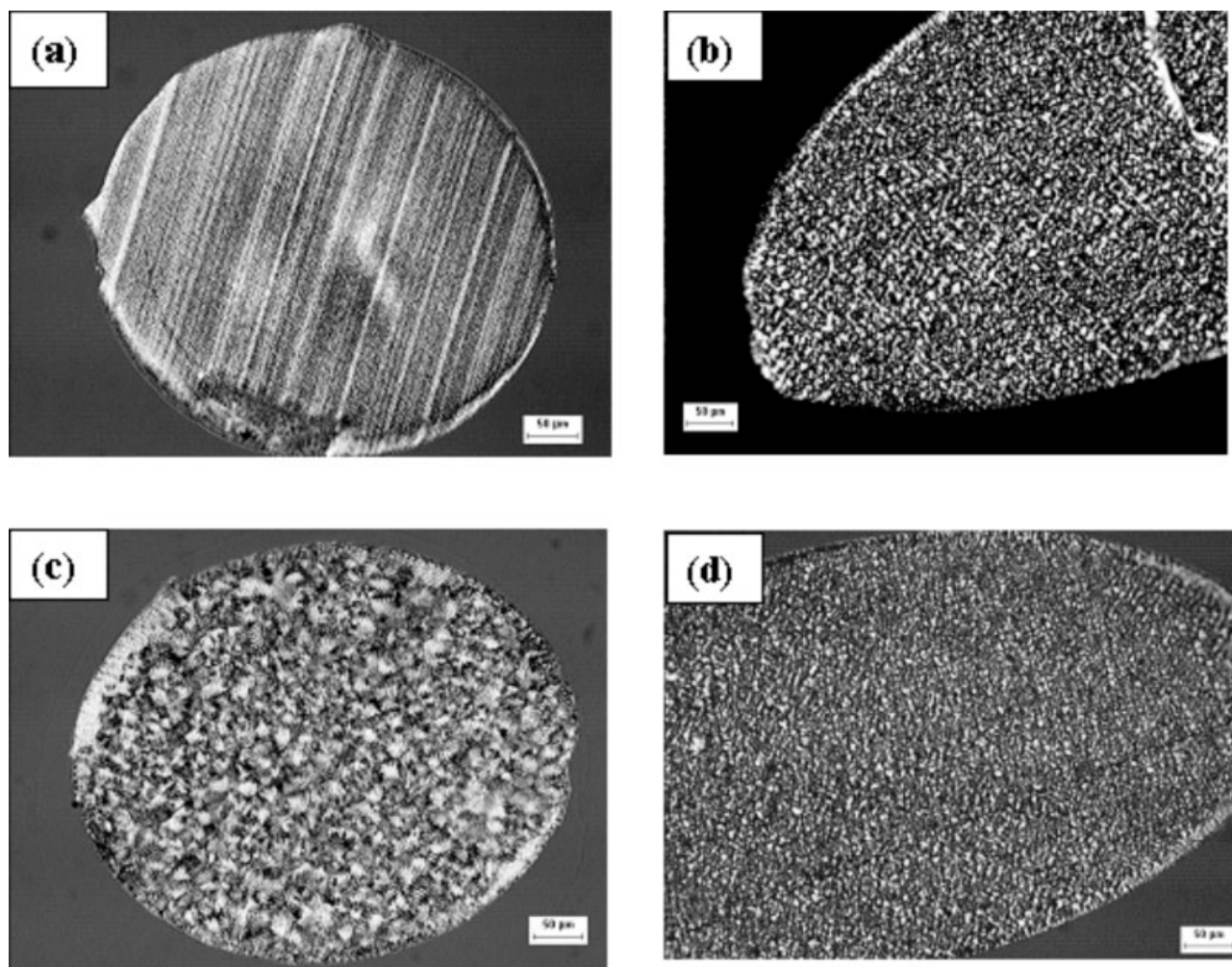


**Figure 3** Cross section of PE1 cylinders under polarizing microscope with  $\times 200$ . (a) Quenched cylinder; (b) air-cooled cylinder; (c) slow-cooled cylinder; (d) air-cooled cylinder after annealing.

ciably with changing the thermal history of the specimen. Figure 2 shows the DSC thermograms for the three resins exposed to different thermal histories. From Figure 2(a), the higher melting temperatures of the slow-cooled samples and annealed samples, all produced from PE1, suggest that more stable crystalline structures (i.e., structure containing fewer defects), or thicker lamellae were formed.<sup>27,28</sup> The sharp onset of melting of the slow-cooled samples suggests a crystalline structure with a lower amount of defects. Thicker lamella and stable crystalline structure probably contributed to higher melting temperature and heat of fusion for PE1 samples exposed to slow cooling rates. On the basis of WAXS measurements, it was found that air-cooled samples had larger crystallites than quenched samples (Table III), indicating that a more stable crystalline structure was formed. DSC results obtained for specimens prepared using PE2 are presented in Figure 2(b). The shoulder of the DSC curves observed for both quenched and air-cooled cylinders is typically seen with resins having high comonomer con-

tent. The broader melting range of air-cooled samples indicates that primarily two types of crystalline structures were formed during cooling. The slow cooling rate (air cooled samples) somewhat allowed for the short ethylene sequences to crystallize at low temperatures. The shoulder seen on the DSC curve for the quenched samples represents the recrystallization of imperfect crystallites formed under a fast cooling rate. As for mPE3 cylinders, the three DSC heating traces [Fig. 2(c)] have very similar shape due to the uniform MWD and comonomer distribution and thus uniform crystalline structure formed during the solidification process.

Annealing treatments are known to enhance the effect of thermal treatments on polymer morphology. The increases in the melting temperature and heat of fusion observed for the three resins exposed to annealing treatments are attributed to an increase in the lamellar thickness and thus thermal stability of lamellar crystals<sup>29,30</sup> rather than changes in the crystallite sizes of ethylene copolymers. Thermal segregation was detected in specimen subjected to annealing treat-

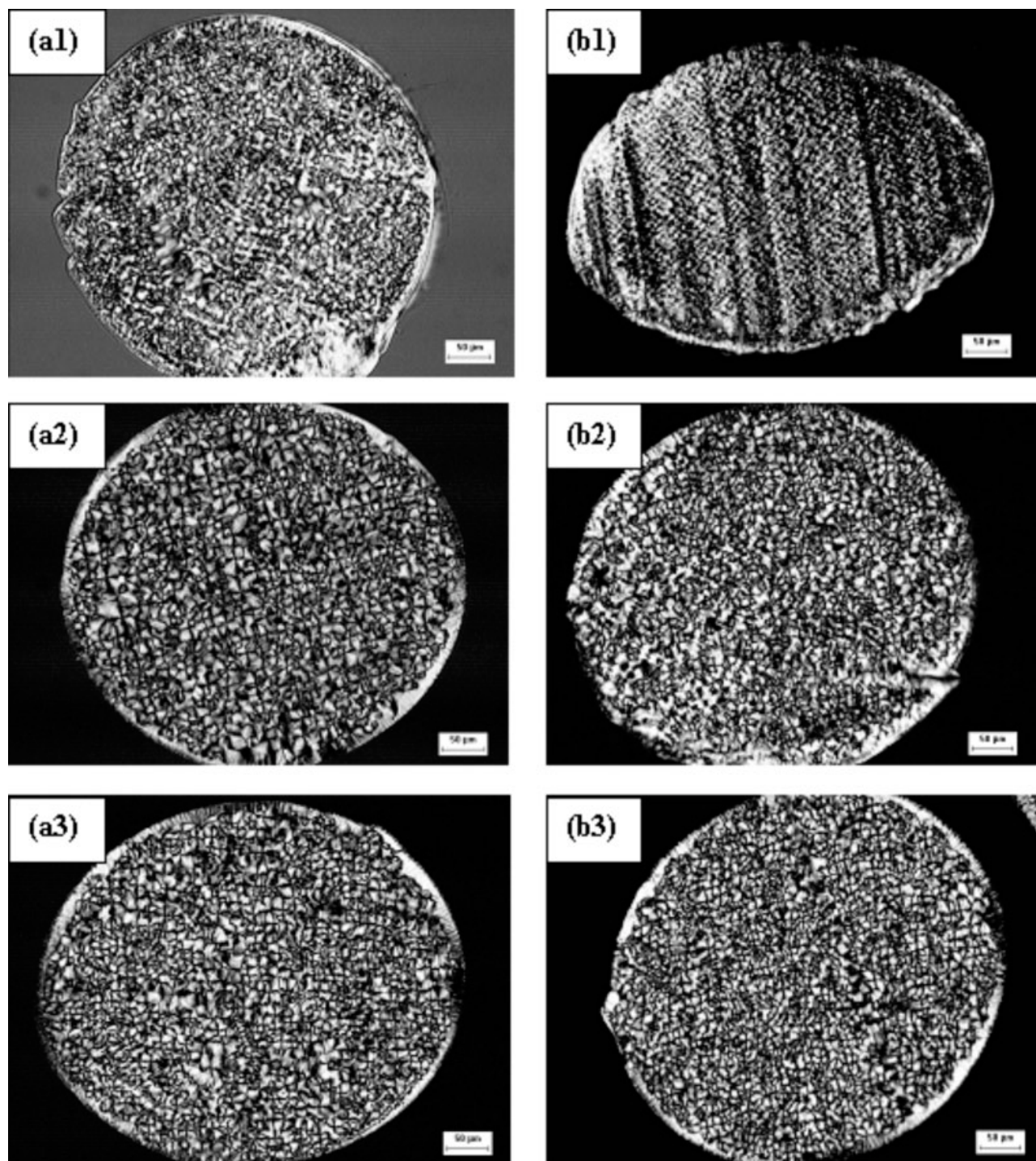


**Figure 4** PLM micrographs of cross sections of cylinders with different thermal treatments. (a1), (a2), and (a3): PE2 quenched, air-cooled, and annealed, respectively; (b1), (b2), and (b3): mPE3 quenched, air-cooled, and annealed, respectively.

ments. Annealed specimens showed narrower melting range for the main endothermic peak, which indicates the formation of crystals with uniform size. The secondary peaks correspond to crystallites having a lower degree of stability, formed from chains having shorter linear ethylene segments. The effect of annealing treatment is more prominent for PE1 and PE2 (Ziegler–Natta catalyzed) than mPE3 (single site cata-

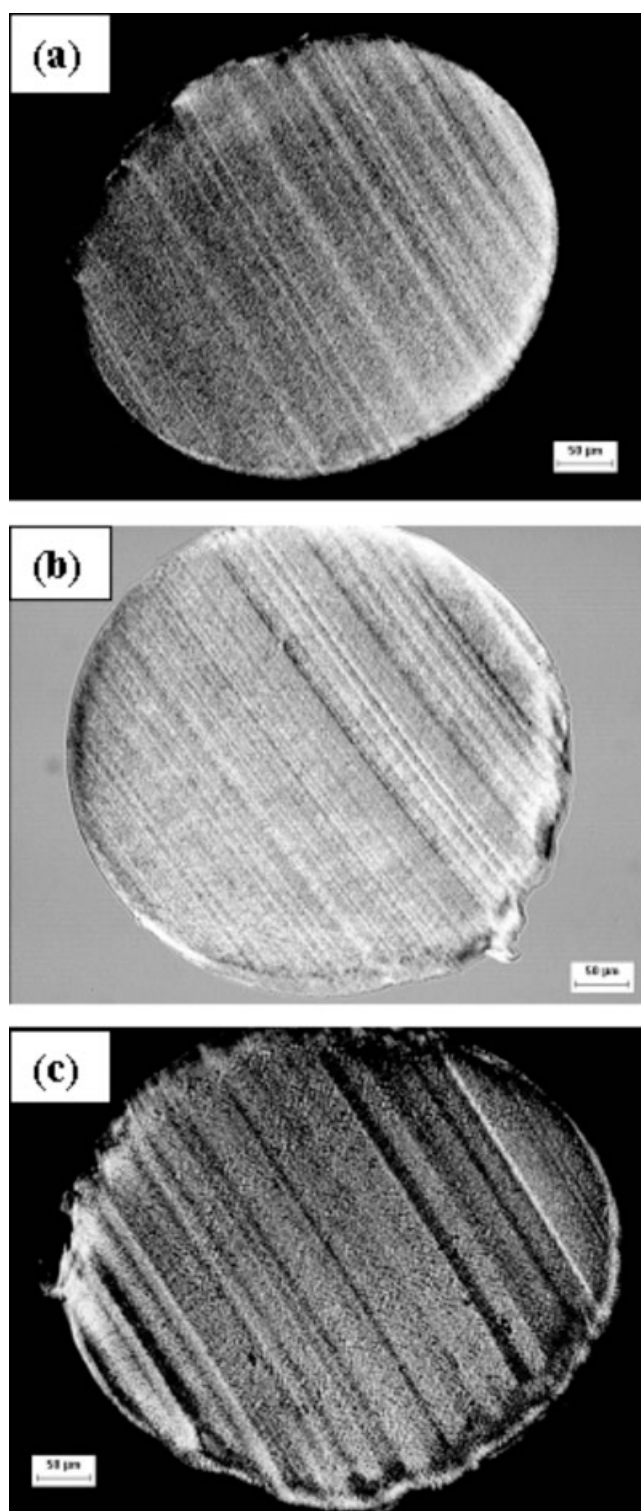
lyzed) due to the difference in the homogeneity in the comonomer distribution.<sup>31</sup>

Figure 3 presents polarized light microscopy (PLM) photographs, which show the crystalline textures of PE1 cylinders under different thermal treatments. The spherulites are very small and cannot be clearly identified in quenched samples. In the air-cooled samples, the spherulites are small but recognizable, while in

the slow-cooled samples, large and well-defined spherulites are observed. PLM photographs of the other two copolymers are shown in Figure 4. All air-cooled samples show large and well-defined spherulites. We attribute the higher melting temperature and heat of fusion of annealed cylinders to the formation of thicker lamellae and stable crystalline structures. The results presented earlier illustrate how the morphology is affected by the material molecular structure and the thermal history. Ziegler–Natta catalyzed copolymers have broader crystallite size distributions than the single site copolymer. Variations in the cooling conditions have important repercussions on the material morphology (spherulite size and stability of crystalline structure), being more noticeable with Ziegler–Natta copolymers.

#### Effect of nucleating agent

Results available in the literature suggest that sorbitol is one of the most effective nucleating agents for polyethylene.<sup>32</sup> Sorbitol-based nucleating agents have a unique mode of action that they can form a fibrous network, which becomes the nucleation site for crystallization, this mechanism enabling them to be very effective morphology modifiers.<sup>33–35</sup> Our experimental results show that the addition of DMDBS affected both the supermolecular structure (Fig. 5) as well as the melting and crystallizing behaviors of ethylene copolymers, as shown in Table III. Both Ziegler–Natta and metallocene resins show a dramatic drop in their spherulite size. The presence of DMDBS increases the number of effective nuclei, and the nucleation rate becomes more predominant than the spherulitic growth rate.<sup>36</sup> The crystallite size, on the other hand, did not change much after the addition of DMDBS (Table III). The bulk crystallinity, the melting temperature, and crystallization temperature all increased with the addition of DMDBS. The increase in the melting temperature indicates that more stable crystalline structures were formed. This may be the result of a decrease in the surface energy since low energy molecular structures form between nucleating agents and polymer molecules. The presence of DMDBS also reduced the undercooling by shifting the crystallization temperature to higher value. This change has likely influenced the stability of the crystalline structure since smaller undercooling generally lead to the formation of thicker lamellae.<sup>37</sup> The addition of DMDBS has, however, resulted in broadening the melting range for PE1 and PE2 (Fig. 6). The single site catalyzed ethylene copolymer (mPE3), on the other hand, showed similar melting behavior with and without the addition of DMDBS. This result suggests that the effect of DMDBS on the nucleation and crystallization kinetics is dependent on the molecular structure of polymers.



**Figure 5** PLM micrographs for cross sections of air-cooled cylinders with the addition of DMDBS. (a) PE1; (b) PE2; (c) mPE3.

#### Coalescence behavior

##### Effect of thermal treatment

The effects of thermal treatment on the coalescing behavior of PE1, PE2, and mPE3 are presented in



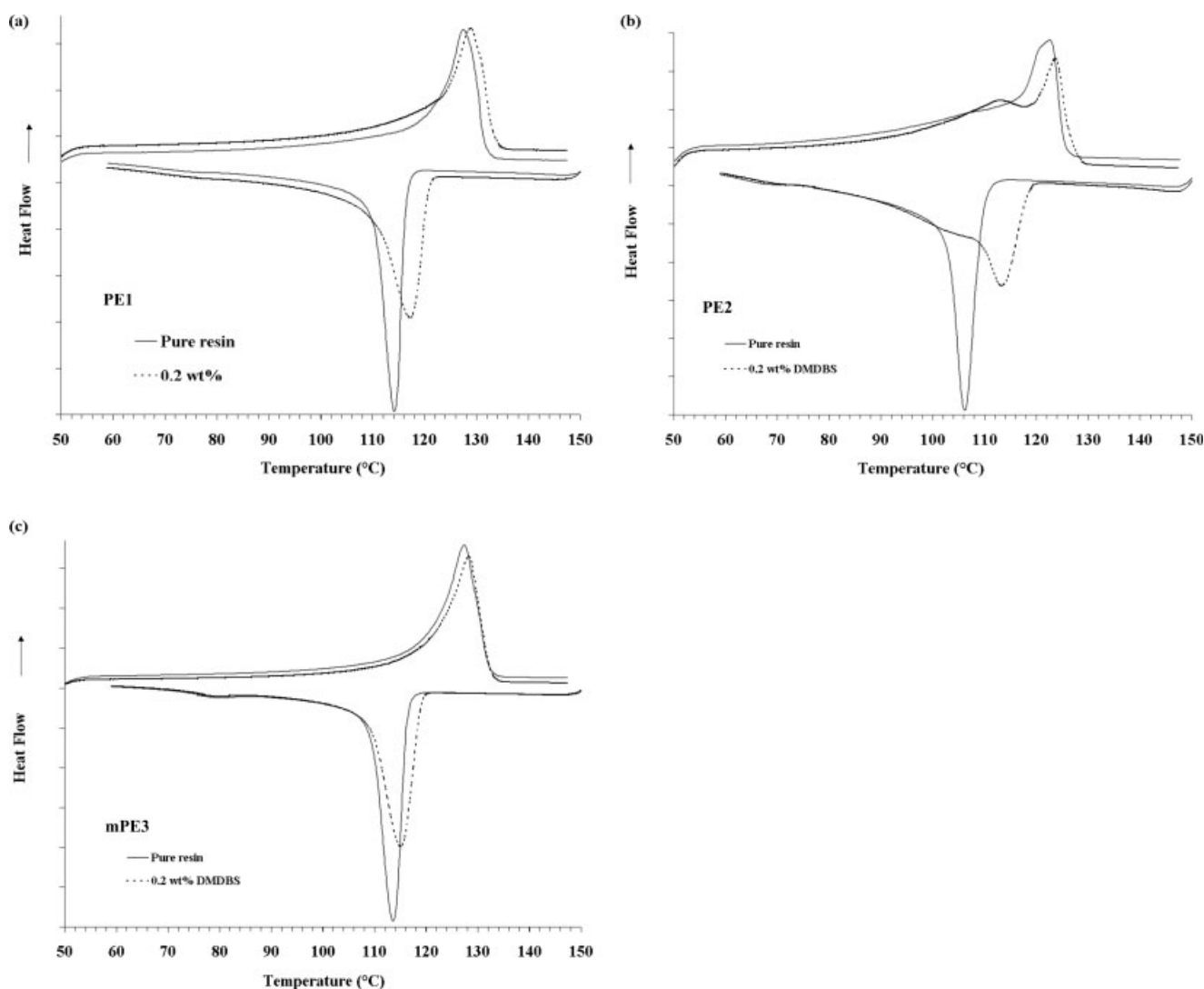
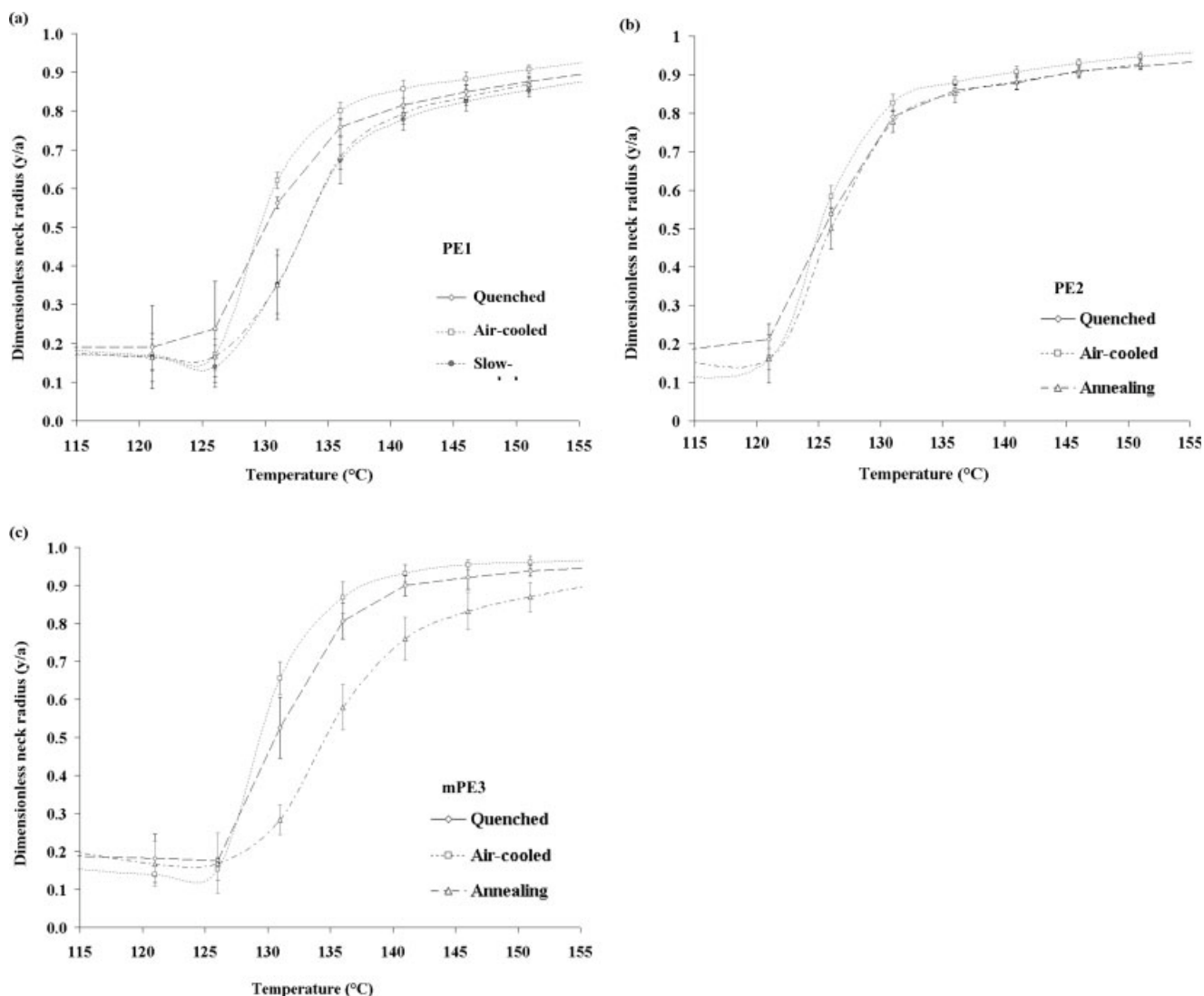


Figure 6 Effects of DMDBS on melting and crystallization of (a) PE1; (b) PE2; (c) mPE3.

Figure 7. Test results show that air-cooled cylinders produced from the three resins considered in this work all show a slightly faster coalescence rate, compared with that obtained with quenched specimens. Air-cooled cylinders have a higher degree of crystallinity and possibly a higher surface tension than the quenched samples.<sup>38</sup> Since surface tension is the driving force in the coalescence process, a higher crystallinity might have favored a faster coalescing rate. More important, however, is the reduction in the coalescence rates of the annealed specimens for PE1 and mPE3, as well as slow-cooled cylinders for PE1, compared with quenched specimens, despite the differences in their crystallinity. Slow cooling and annealing treatments lead to the formation of thick lamellae and crystalline structures with increased stability. In the rotational molding process, the coalescence phenomenon occurs at a temperature range very close to the melting point of the material. Under such condi-

tions, the polyethylene melt may exhibit some structural order, not unlike that seen in liquid crystal polymers.<sup>39–42</sup> The presence of crystalline structures with high stability would have an impact on the volume fraction as well as stability of the ordered component present in the molten phase. Accordingly, this would influence the chain mobility and slow down molecular diffusion at a temperature range close to that of the melt transition and thus cause a reduction in the coalescing rate observed for annealed specimens.

Variations in the thermal treatment imposed on coalescing particles produced from PE2 did not result in changes in their coalescing behavior as important as those observed for PE1. This resin has a low viscosity and high comonomer content when compared with other resins used in this work. The low viscosity favors a fast coalescing rate, which probably dominates over other effects. Ethylene copolymers with



**Figure 7** Effects of thermal treatment on the coalescence behavior of cylindrical particles for (a) PE1; (b) PE2; (c) mPE3.

higher comonomer content are also less sensitive to variations in thermal treatments.<sup>11</sup>

#### Effect of nucleating agent

Figure 8 presents the coalescence results for three resins before and after the addition of DMDBS. The addition of nucleating agent caused changes in the coalescence behavior of the three resins, the two Ziegler–Natta catalyzed copolymers (PE1 and PE2) being affected more severely than the single site catalyzed resin (mPE3). The effect of adding DMDBS on the coalescing behavior is also illustrated in Figure 9, which displays the coalescence sequence of PE2 cylinders of both pure and addition of DMDBS. From the top view, cylindrical particles of pure resin coalesce faster than those of compound with DMDBS. The side view gives better indication of the polymer melt contour evolution with temperature. The melted particles of

PE2 compounded with DMDBS show slow movement in their contour and retain their initial disk shape for a longer period of time.

The DMDBS was effective in changing the spherulitic size and crystallization behavior for the three copolymers considered in this work. While the degree of crystallinity increases with the presence of the nucleating agent, the addition of a low molecular weight and low surface energy molecule (DMDBS) to the polymer might have resulted in lowering the surface tension of the blend. However, such changes are expected to be small considering the low amount of DMDBS present in the blend (0.2 wt %). Moreover, results obtained from contact angle experiments conducted on solid material did not show conclusive changes in the surface energy with changes in the material composition.<sup>43</sup> The effect of DMDBS on the coalescence behavior, however, is limited to PE1 and PE2. The addition of DMDBS to the Ziegler–Natta cat-

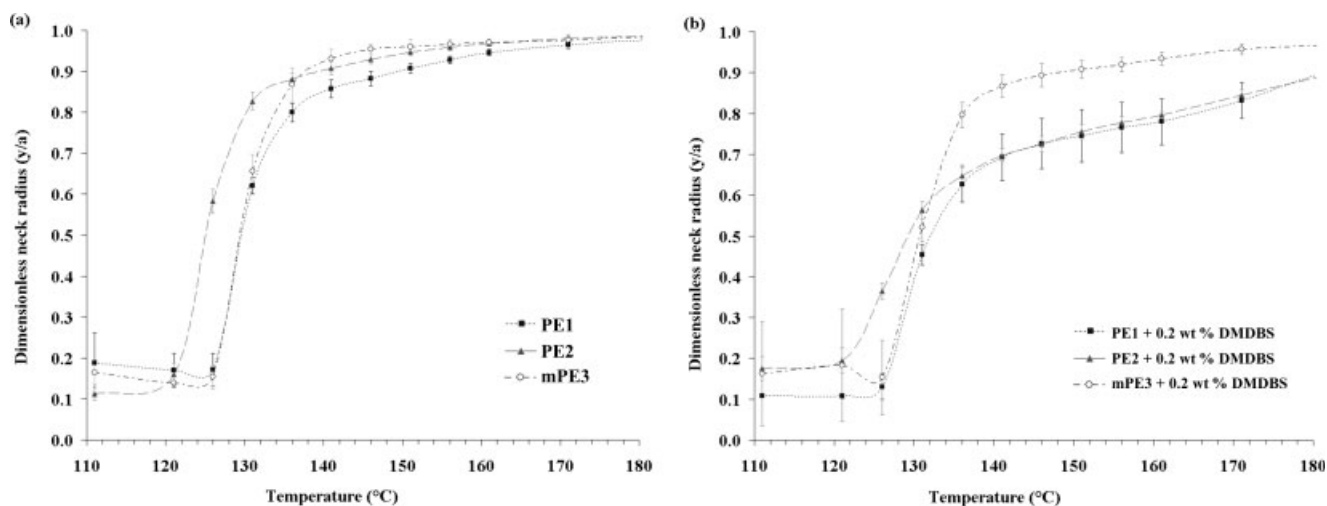


**Figure 8** Effects of DMDBS on the coalescence behavior of air-cooled cylinders for different ethylene copolymers. (a) Pure resins; (b) 0.2 wt % DMDBS blend.

alyzed resins was effective in increasing the stability of the crystallites. This, in turn, may have contributed to lowering the mobility of the polymer chains and slowing the coalescing rate. Figure 10 presents the dynamic viscosity of three resins under temperature sweep oscillatory measurements. With the addition of DMDBS, the crystallization temperatures and the viscosity of PE1 and PE2, the two Ziegler–Natta catalyzed resins, shifted to higher values. The increased viscosity at the temperature near the melting temperature indicates the formation of physical gels, a phenomenon which has been observed in sorbitol nucleated compounds.<sup>18,33</sup> These results show that nucleated

specimens prepared from PE1 and PE2 have reduced chain mobility, compared with the pure resins. On the other hand, the viscosity of the metallocene-based resin, mPE3, did not change appreciably with the addition of DMDBS, which would explain the less important effect seen on the coalescing behavior for this resin.

Although the addition of DMDBS affected the morphology of all three resins considered in this work, their coalescence behavior can better be explained from results obtained from both thermal and rheological characterization of the DMDBS compounds. The addition of DMDBS to the Ziegler–Natta resins has

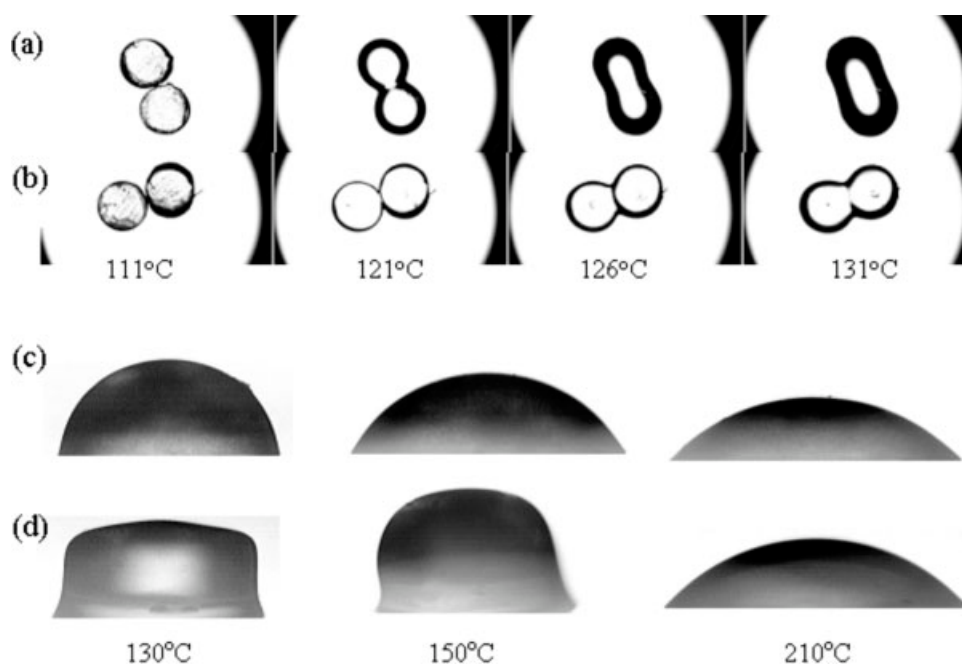


**Figure 9** Coalescence sequence of PE2 cylinders: (a) top view of pure resin; (b) top view of 0.2 wt % DMDBS blend; (c) side view of pure resin; (d) side view of 0.2 wt % DMDBS blend.

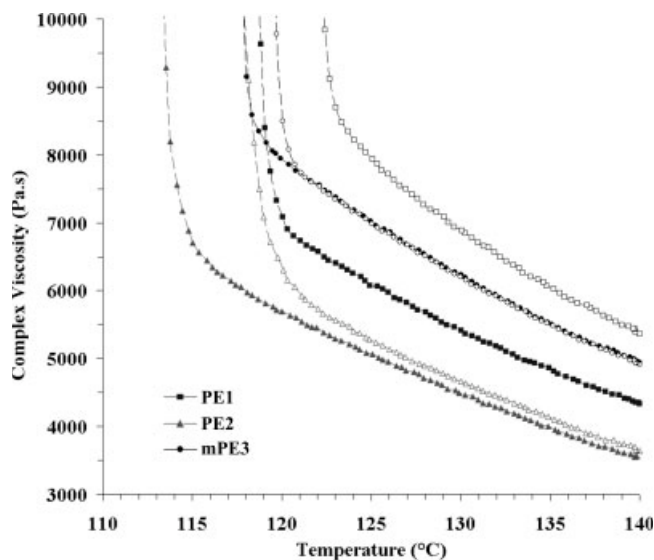


**Figure 10** Viscosity changes for pure resins and blends near crystallization point: filled symbols denote pure resins; empty symbols denote resins with 0.2 wt % DMDBS.

resulted in the formation of crystalline structure with a broader range of stability (Fig. 6), and reduced molecular mobility. Such changes in the stability of the crystalline structure and chain mobility were insignificant for the metallocene catalyzed resin. Changes in the molecular mobility were explained by the formation of submicron-sized structure formed with the presence of the sorbitol additive, which manifest themselves in the increase in the complex viscosity at temperatures near the melt crystallization transition. This suggest the presence of ordered structure at temperatures above the melting point of the material, a question that has long been debated but which is supported by increasing evidence from rheological and interfacial tension, and NMR studies.<sup>39–42</sup> The formation of such structures, however, is dependent on the molecular structure of the resin, as suggested by our results. Heterogeneities in the molecular weigh distribution and, more importantly, comonomer distribution seen in the Ziegler–Natta favor the formation of physical gels in the presence of DMDBS, thus a reduction in the chain mobility near the melting transition and a reduction in the coalescing behavior of the blends.

## CONCLUSIONS

In this work, we have investigated the effects of changes to the material formulation and thermal history on the particle morphology and coalescence behavior of ethylene copolymers. Variations in the thermal treatment during the preparation of samples were found to have some effect on the degree of crystallinity, size of crystals, and characteristics of the

supermolecular structure. The impact of thermal treatment on the coalescence behavior, however, was limited. This may due to the relatively small level of change in the sample's crystalline structure compared to the material viscosity, a property which very much dictates the coalescence behavior of polymers. The addition of a sorbitol nucleating agent (DMDBS) to the material, on the other hand, had an important impact on the morphology of the three resins considered in this work, but also had a detrimental effect on their coalescence behavior, the latter being more apparent for the Ziegler–Natta copolymers. The reduction in the coalescing rates of polymers with the addition of a nucleating agent was attributed to an increase in the crystalline lamellar thickness and the development of gelation structures, which cause a reduction in the chain mobility near the melting temperature. The formation of such structures, however, is dependent on the molecular structure of the copolymers and may be favored by the presence of heterogeneities in the comonomer distribution.

It is important to understand how the coalescence behavior is affected by changes in the formulation of polymers used for rotational molding applications. Resins with low coalescing rates require longer exposure at high temperatures for the completion of the densification process. Long heating cycles are not only detrimental to the economics of the process, but also favor degradation reactions which in turn are detrimental to the properties of the end-products. The addition of additives, such as pigments, fillers, and nucleating agents, is a common practice for the improvement of optical and mechanical properties of end products. Our results showed, however, that caution must be applied as variations in the material composition can lead to changes in the stability of the particles' morphology as well as important repercussions on the coalescence process.

The authors acknowledge Mr. C. Luo, Mr. K. Kuklisin, and Ms. T. Huynh of NOVA Chemicals Corporation for their help on the X-ray diffraction test and dynamic mechanical analysis; and thank Dr. J. W. Teh for valuable discussion.

## References

- Oliveira, M. J.; Cramez, M. C.; Crawford, R. J. *J Mater Sci* 1996, 31, 2227.
- Oliveira, M. J.; Cramez, M. C. *J Macromol Sci Phys* 2001, 40, 457.
- Cramez, M. C.; Oliveira, M. J.; Crawford, R. J. *J Mater Sci* 2001, 36, 2151.
- Mathot, V. B. F.; Scherrenberg, R. L.; Pijpers, T. F. J. *Polymer* 1998, 39, 4541.
- Crist, B.; Howard, P. R. *Macromolecules* 1999, 32, 3057.
- Chum, S.; Stephens, C. H.; Poon, B.; Ansems, P.; Hiltner, A.; Bear, E. *SPE ANTEC* 2003, 49, 1775.
- Simanke, A. G.; Galland, G. B.; Freitas, L.; da Jornada, J. A. H.; Quijada, R.; Mauler, R. S. *Polymer* 1999, 40, 5489.

8. Wang, C.; Chu, M.-C.; Lin, T.-L.; Lai, S.-M.; Shih, H.-H.; Yang, J.-C. *Polymer* 2001, 42, 1733.
9. Zhang, F.; Song, M.; Lü, T.; Liu, J.; He, T. *Polymer* 2002, 43, 1453.
10. Zhang, F.; Liu, J.; Xie, F.; Fu, Q.; He, T. *J Polym Sci, Part B: Polym Phys* 2002, 40, 822.
11. Peeters, M.; Goderis, B.; Vonk, C.; Reynaers, H.; Mathot, V. *J Polym Sci, Part B: Polym Phys* 1997, 35, 2689.
12. Mandelkern, L.; Glotin, M.; Benson, R. A. *Macromolecules* 1981, 14, 22.
13. Bensason, S.; Minick, J.; Moet, A.; Chum, S.; Hiltner, A.; Baer, E. *J Polym Sci, Part B: Polym Phys* 1996, 34, 1301.
14. Peeters, M.; Goderis, B.; Reynaers, H.; Mathot, V. *J Polym Sci, Part B: Polym Phys* 1999, 37, 83.
15. Starck, P. *Polym Int* 1996, 40, 111.
16. Feng, Y.; Jin, X.; Hay, J. N. *J Appl Polym Sci* 2089, 1998, 69.
17. Smith, T. L.; Masilamani, D.; Bui, L. K.; Khanna, Y. P.; Bray, R. G.; Hammond, W. B.; Curran, S.; Belles, J. J.; Binder-Castelli, S. *Macromolecules* 1994, 27, 3147.
18. Kristiansen, M.; Werner, M.; Tervoort, T.; Smith, P.; Blumenhofer, M.; Schmidt, H.-W. *Macromolecules* 2003, 36, 5150.
19. Mazur, S. In *Polymer Powder Technology*, 1st ed.; German, R. M., Messing, G. L., Cornwall, R. G., Eds.; Wiley: New York, 1995; p 157.
20. Bellehumeur, C. T.; Bisaria, M. K.; Vlachopoulos, J. *Polym Eng Sci* 1996, 36, 2198.
21. Bellehumeur, C. T.; Kontopoulou, M.; Vlachopoulos, J. *Rheol Acta* 1998, 37, 270.
22. Siegmann, A.; Raiter, I.; Narkis, M.; Eyerer, P. *J Mater Sci* 1986, 21, 1180.
23. Barnetson, A.; Hornsby, P. R. *J Mater Sci Lett* 1995, 14, 80.
24. Guillén-Castellanos, S. A.; Lin, W.; Bellehumeur, C. T.; Weber, M. *Int Polym Process* 2003, 18, 87.
25. Rezaei, M.; Ebrahimi, N. G.; Kontopoulou, M. *Polym Eng Sci* 2005, 55, 678.
26. Takacs, E.; Bellehumeur, C. T.; Vlachopoulos, J. *Rotation* 1996, 5, 17.
27. Androsch, R. *Polymer* 1999, 40, 2805.
28. Fernández, C.; Puig, C. C. *J Macromol Sci Phys* 2002, 41, 991.
29. Peeters, M.; Goderis, B.; Reynaers, H.; Mathot, V. *J Polym Sci, Part B: Polym Phys* 1998, 37, 83.
30. Alizadeh, A.; Richardson, L.; Xu, J.; McCartney, S.; Marand, H.; Cheung, Y. W.; Chum, S. *Macromolecules* 1999, 32, 6221.
31. Adisson, E.; Ribeiro, M.; Deffieux, A.; Fontanille, M. *Polymer* 1992, 33, 4337.
32. Kurja, J.; Mehl, N. A. In *Plastics Additives Handbook*, 5th ed.; Zweifel, H., Ed.; Hanser Publishers: Munich, 2001; p 960.
33. Shepard, T. A.; Delsorbo, C. R.; Louth, R. M.; Walborn, J. L.; Norman, D. A.; Harvey, N. G.; Spontak, R. J. *J Polym Sci, Part B: Polym Phys* 1997, 35, 2617.
34. Bauer, T.; Thomann, R.; Mülhaupt, R. *Macromolecules* 1998, 31, 7651.
35. Thierry, A.; Straupe, C.; Lotz, B.; Wittmann, J. C. *Polym Commun* 1990, 31, 299.
36. Wunderlich, B. *Macromolecular Physics*, Vol. 1; Academic Press: New York, 1973; p 193.
37. Marco, C.; Gómez, M. A.; Ellis, G.; Arribas, J. M. *J Appl Polym Sci* 2002, 84, 1669.
38. Wu, S. *Polymer Interface and Adhesion*; Marcel Dekker: New York, 1982; p 76.
39. Kamel, I.; Charlesby, A. J. *J Polym Sci Polym Phys Ed* 1981, 19, 803.
40. Bremner, T.; Rudin, A. *J Polym Sci, Part B: Polym Phys* 1992, 30, 1247.
41. Hussein, I. A.; Williams, M. C. *Macromolecules* 2000, 33, 520.
42. Chan, C. C. V.; Elliot, J. A. W.; Williams, M. C. *J Appl Polym Sci* 2003, 90, 4061.
43. Lin, W. M.Sc. Thesis, University of Calgary, Calgary, AB, Canada, 2003.